An Exploratory Multi-Session Study of Learning High-Dimensional Body-Machine Interfacing for Assistive Robot Control

Jongmin M. Lee[1,2,Ψ], Temesgen Gebrekristos[1,2], Dalia De Santis[2], Mahdieh Nejati-Javaremi[1,2], Deepak Gopinath[1,2], Biraj Parikh[1], Ferdinando A. Mussa-Ivaldi[1,2], and Brenna D. Argall[1,2]

***Abstract*— Individuals who suffer from severe paralysis often lose the capacity to perform fundamental body movements and everyday activities. Empowering these individuals with the ability to operate robotic arms, in high degrees-of-freedom (DoFs), can help to maximize both functional utility and independence. However, robot teleoperation, in high DoFs, currently lacks accessibility due to the challenge in capturing high-dimensional control signals from the human, especially in the face of motor impairments. Body-machine interfacing is a viable option that offers the necessary high-dimensional motion capture, and it moreover is noninvasive, affordable, and promotes movement and motor recovery. Nevertheless, to what extent body-machine interfacing is able to scale to high-DoF robot control, and whether it is feasible for humans to learn, remains an open question. In this exploratory multi-session study, we demonstrate the feasibility of human learning to operate a body-machine interface to control a complex, assistive robotic arm. We use a sensor net of four inertial measurement unit sensors, bilaterally placed on the scapulae and humeri. After calibration, ten uninjured participants are familiarized, trained, and evaluated in reaching and Activities of Daily Living tasks, using the body-machine interface. Our results suggest the manner of control space mapping (joint-space control versus task-space control), from interface to robot, plays a critical role in the evolution of human learning. Though joint-space control shows to be more intuitive initially, task-space control is found to have a greater capacity for longer-term improvement and learning. This seems to come at a cost, however, where perceived workload presents to be a bigger challenge for task-space control, compared to joint-space control.**

I. Introduction

People who suffer from upper and/or lower body paralysis experience loss of functional independence, and cascading effects further disrupt quality of life [1]. Even with cervical spinal cord injury (cSCI), people can restore voluntary mobility using assistive robots. Assistive robots that are functional, intuitive, and learnable maximize opportunities for movement and independence to be restored [1]. While there are many strategies to support patients with robots, technologies that empower patients to directly teleoperate complex robots offer the freedom to achieve everyday tasks with independence [2].

There are several examples of robotic platforms with the capability and control complexity to allow patients to perform Activities of Daily Living (ADLs) via direct control [3]. However, the robotics community has yet to truly overcome the dimensionality mismatch problem that exists between control interfaces and complex assistive robots [4]. That is, there lies a mismatch between the number of control signal dimensions that a single commercially-available assistive interface (e.g., sip-and-puff, limited-throw joystick) is capable of issuing , in comparison to the number of degrees-of-freedom (DoF) required for complex robot control . Unfortunately, simultaneous and continuous robot control in all translation and orientation dimensions has been extremely challenging with conventional interface solutions. This is critical because high control complexity is often needed in order for patients to achieve high-resolution dexterous movements in our physical world—and to efficiently perform everyday tasks, with intention, in a timely manner.

The problem of dimensionality mismatch and making high-resolution control accessible to patients can potentially be overcome using Body-Machine Interfaces (BoMIs). BoMIs use motion sensor technologies to measure movement from the surface of the body [5]. Relative to the aforementioned commercially-available interfaces, BoMIs have the capacity to generate control signal inputs in higher dimensions, from residual body movements [6]

Moreover, movement training and therapy that encourage residual movements and mobility are shown to promote neuroplastic changes and improve functionality [7]. BoMIs incentivize patients to use their remaining residual mobility to produce control inputs [8].

Thus, in addition to overcoming dimensionality mismatch, there are deeper implications that extend beyond assistance through robotics—that is, BoMIs also promote physical therapy and rehabilitation [9].

A current challenge with BoMIs is that there is a limited understanding of the extent to which people can learn to recoordinate their body movements, to issue high-dimensional signals, *necessary* to simultaneously control all of the DoFs of a complex robot. Prior studies have raised concerns that BoMI control could possibly be unintuitive and/or difficult to learn as control complexity in the robot increases [10]. In addition, the question of whether body movements can be executed—with consistency and sufficient dexterity—to complete functional tasks via direct BoMI control remains unanswered.

We take steps to address this challenge with an exploratory investigation of complex robotic arm operation via a high-dimensional BoMI. More specifically, in this paper, we make the following contributions:

- A presentation of a multi-session study of high-DoF robotic arm teleoperation via a high-dimensional BoMI.

[1]Northwestern University, Evanston, Illinois, USA.
[2]Shirley Ryan AbilityLab, Chicago, Illinois, USA.
[Ψ]Corresponding author: jmlee@u.northwestern.edu.

- A demonstration that body machine interfacing is feasible and scalable to higher-DoF robots within a loosely-structured learning environment.
- An analysis of the impact of control space mappings (control in task space versus joint space) on task performance, workload, and human learning.

The remainder of the paper is organized as follows. We summarize related literature in Section II. The methods of our multi-session study and its analysis are presented in Section III. The results of the study are reported in Section IV, with further discussion within Section V. In Section VI, we provide our conclusions.

II. Related Work

A common solution to dimensionality mismatch is modal control [11], in which only a subset of the control dimensions of the robot are operated at a given time. While modal control does facilitate access to the full control space, it does not allow people to access all control dimensions simultaneously and can lead to increases in time, cognitive load, and errors, when they attempt to perform tasks with complex robots [11].

Interfaces such as Brain-Machine Interfaces (BMIs), using implants, offer the possibility of directly issuing high-dimensional control signals to overcome the problem of dimensionality mismatch and bypass the need for modal control. Although BMIs have enormous potential to help people with neurological disorders and injuries, including cSCI, they can be extremely invasive—requiring surgery to the brain and the permanent implantation of an electrode array [12]. Though BMI can be noninvasive using surface electroencephalography (EEG), there is less evidence that suggests the signal-to-noise ratio is sufficient for the continuous and simultaneous control of robots in high DoFs [13].

A similar potential, to directly control in high DoFs, exists in BoMIs. Even in tetraplegia, residual body movements can remain intact [14], and BoMIs are able to capitalize on these residual movements available to patients with paralysis. They are responsive to patient-to-patient variability (e.g., between or within levels of SCI) [5], enhance muscle strength and mobility [6], and achieve functional rehabilitation aims [9]. By casting a net of sensors on the body, the BoMI captures body movements. In general, BoMIs can be customized to individuals through their particular availability of body movements; for example, by tuning the BoMI map's parameters (e.g., gains, offsets) session-by-session [6]. A classic approach to designing a BoMI map is to describe a linear relationship between sensor measurements and robot control commands [6]. More recent examples use iterative linear methods [15], feedback control (as opposed to feedforward control) [16], and deep learning methods such as adaptive nonlinear autoencoders [17].

BoMIs are interfaced with a variety of assistive platforms, including powered wheelchairs [18] and robotic arms [19]—for all of which the control output is either discrete or the maximum continuous controllable dimensions are fewer than three. Using a BoMI for higher-DoF control of assistive robots remains an open research question.

III. Methods

Here we present the experimental details of our multi-session study of robotic arm operation using a high-dimensional BoMI (Figure 1).

Participants. A total of ten uninjured adults (median age 28 ± 8 years; 6 males, 4 females) were recruited to participate in this study. Each participant completed five sessions of approximately two hours each, across five consecutive days. Participants were assigned to one of two groups based on control space mappings: task-space (TS) or joint-space (JS). The TS group controlled the velocity of the robot end-effector in translation and orientation, while the JS group controlled the velocity of the robot joints. Group assignment was random and balanced such that participants of each group received the same tasks, number of trials, and number of sessions. All sessions were conducted with the approval of the Northwestern University Institutional Review Board (STU00210069). All participants provided their written informed consent.

Body-Machine Interface. A sensor net consisting of four inertial measurement unit (IMU) sensors (Yost Labs, Ohio, USA) were placed bilaterally on the scapulae and humeri, and anchored to a custom shirt designed to minimize movement artifacts. Sensor placement was adopted from past BoMI studies [6]. To maintain consistency between participants, we used orientation data from an additional reference chest sensor through a predetermined kinematic chain (chest $\rightarrow$ shoulders $\rightarrow$ upper arms). A Kalman filter was used as the filtering method for the IMUs, where orientation data was computed in real-time, onboard the IMU sensors, through a fusion of accelerometer and gyroscope measurements.

The pipeline and decoder design are visually represented in Figure 1b (top). The relative quaternion orientations of the four IMUs in the net (16D) were mapped (similar to [6]) to a 6D linear subspace using Principal Component Analysis (PCA). Initially, PCA was used to precompute a map ($\mathbf{A}$) and an affine offset ($\mathbf{b}_0$), using data collected from an experienced user, performing a predefined set of upper body movements (shoulder elevation/depression, protraction/retraction, elbow abduction/adduction). The PCA map allowed for a linear mapping between the 16D orientation data signal ($\mathbf{x}$) and a 6D control signal ($\mathbf{q}$) as: $\mathbf{q} = \mathbf{A}\mathbf{x} + \mathbf{b}_0$.

Robot Control. The lower-dimensional PCA subspace was used online to control a 7-DoF JACO robotic arm (Kinova Robotics, Quebec, Canada) with the fifth joint held fixed—which was the redundant joint in its kinematic chain. We held this joint fixed so that both of the control-space-mapping groups (TS and JS) were operating the same number (6) of DoFs, and under the same control constraints.

The principal components (PCs) of the lower-dimensional PCA subspace were mapped to the robot control space as follows. For the TS group, we prioritized control in translation over control in orientation by mapping the first three PCs (which by definition capture more body movement variance than the three latter PCs) to position (x, y, z) velocities, and

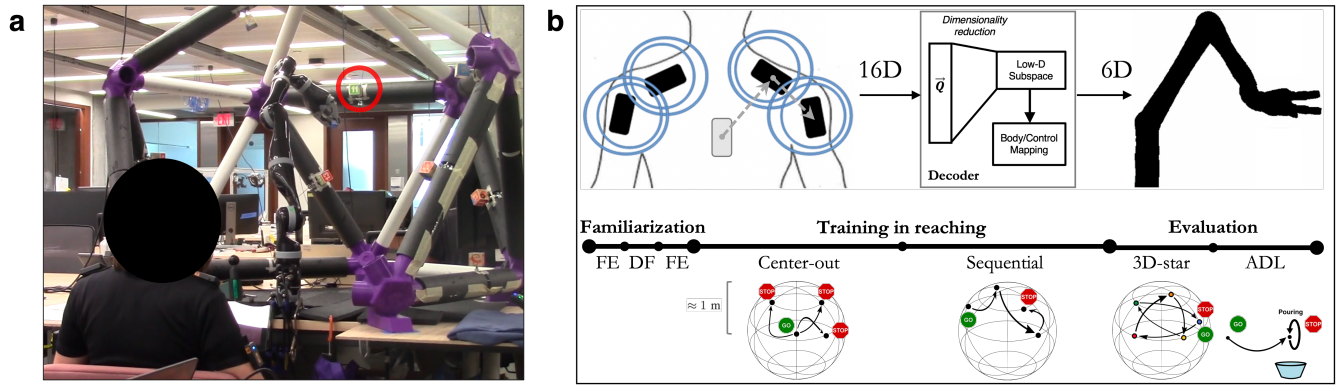

Fig. 1: Overview of the interface-robot pipeline and study tasks. (a) Participant wearing the BoMI and operating the JACO robotic arm. Reaching targets affixed to a custom-built cage. (b) *Top*: BoMI IMUs (16D = 4 IMUs × 4D quaternion), mapped to a 6D linear subspace for continuous and simultaneous control of the robot in task-space (3D translation + 3D orientation) or joint-space (6D joint angles). *Bottom*: Progression of study session tasks: (1) free exploration (FE); (2) all-but-one DoF freezing (DF); (3) FE; (4) center-out reaching; (5) sequential reaching; (6) sequential reaching in a 3D-star shape; (7) ADL-inspired tasks.

the next three PCs to orientation (θ roll, ϕ pitch, ψ yaw) velocities. For the JS group, we mapped the PCs in the order of joints in the kinematic chain of the robotic arm.

To avoid involuntary robot commands and to compensate for sensor noise during study trials, we used a control threshold formulation, for dead zoning, that was linearly proportional to the applied gains, shifted by a constant offset. To maximize the utility of the map for each individual, we customized the 6D signal ($\mathbf{q}$) to the individual through scaling and shifting of control gains and offsets, determined through observation-based tuning. Control signals to the robot were published at an approximate rate of 100 Hz.

Visual Feedback. A graphical-user interface (GUI) displayed on a tablet provided real-time visualization of the robot velocity commands to the participant. A scoring system also was displayed on the GUI to increase participant engagement and to provide trial-by-trial feedback on performance. Scores were calculated based on robot end-effector distance-to-target. Participants were told that this is a score but were not provided with the calculation details.

Study Protocol. There were three phases of robot operation in the protocol of a single study session (Figure 1b, bottom).

1) **Familiarization**: The *free exploration* (FE) task encouraged participants to explore and become familiar with the system. The *all-but-one DoF freezing* (DF) task iteratively introduced each control dimension, one at a time, while all other DoFs were kept frozen.
2) **Training**: The *center-out reaching* task started always from a fixed center position when reaching targets. The *sequential reaching* task instead began each reach from the prior reach's target position. Ten targets were used as reaching goals, and placements remained fixed throughout the study and across participants. The order of targets was randomized and balanced across days to avoid ordering effects, and this order was preserved across participants. These tasks modelled a standard experimental paradigm in motor learning [20] and movements that are more typical in practice.
3) **Evaluation**: To evaluate *sequential reaching*, participants were presented with five targets, that comprised a three-dimensional star, in fixed succession. To evaluate *ADL* task ability, participants: (a) transfered a cup (upside-down) from a dish rack and placed it (upright) on the table, (b) poured cereal into a bowl, (c) scooped cereal from a bowl, and (d) threw away a surgical mask into a trash bin.

A trial ended upon successful completion or timeout. For a given reach to a target, success was defined within strict positional (1.00 cm) and rotational (0.02 rad, or 1.14°) thresholds, and the timeout was 90 seconds. For the ADL tasks, experimenters followed codified guidelines to determine when tasks were completed with a task timeout of 3 minutes. Over the course of the study, the dataset of all participants and sessions consisted of a total of 400 center-out, 400 sequential, and 250 3D-star reaching trials, as well as from 80 ADL-task trials.

Performance metrics. To evaluate the study's reaching evaluation tasks, we define the following performance metrics:

- Success rate

$$\mu_S = \frac{1}{N}\sum_{n=1}^{N} \mathbf{1}_{\{S\}_n}, \tag{1}$$

where

$$\mathbf{1}_{\{S\}} = \begin{cases} 1, & \text{task success} \\ 0, & \text{otherwise,} \end{cases}$$

N is the total number of trials, and $\mathbf{1}_{\{S\}_n}$ is an indicator function that summarizes task success.

- Successful completion time

$$t_c = \mathbf{1}_{\{S\}}(t_{end} - t_{start}), \tag{2}$$

where t_{start} and t_{end} are the respective start and end times of a given trial.

- Average number of collisions

$$\mu_{collision} = \frac{1}{N}\sum_{n=1}^{N} \mathbf{1}_{\{C\}_n}, \tag{3}$$

where $\mathbf{1}_{\{C\}_n}$ is an indicator function that summarizes task collisions. A collision is marked when any part of the robot comes in contact with the physical environment.

- Normalized path length in a given reach

$$\frac{\ell_{path}}{\ell_{straight}} = \frac{\sum_{m=0}^{M-1} \|\mathbf{x}_m - \mathbf{x}_{m+1}\|^2}{\|\mathbf{x}_{target} - \mathbf{x}_{start}\|^2}, \tag{4}$$

where $\|\cdot\|$ is the L2 norm, and ℓ_{path} and $\ell_{straight}$ are the trial's end-effector path length and straight-line path length, respectively, to a target. M is the total number of samples ($f_s = 10$ Hz), $\mathbf{x}_m$ is the end-effector pose at the m^{th} sample, and $\mathbf{x}_{start} = \mathbf{x}_0$.

- Average proportion of time spent within k percent of reach distance

$$\mu_{\tau_{dist\leq k}} = \frac{1}{N}\sum_{n=1}^{N} \tau_{dist\leq k,n}, \tag{5}$$

$$\tau_{dist\leq k} = \frac{t_{dist\leq k}}{t_{end} - t_{start}},$$

where $k \in [0, 100]\%$. Note, we can substitute $dist \geq 100\%$ to compute this beyond 100% of the reach distance ($\tau_{dist\geq 100\%}$). This metric is used to supplement (low reaching performances in) more traditional task performance metrics (Equations 1, 2, 4).

To evaluate the study's ADL tasks, we use the two success metrics defined above.

Questionnaires. The NASA task load index (NASA-TLX) is an assessment tool to measure subjective workload in human-machine interfacing contexts [21], and is administered at the end of each session.

IV. Results

We report results from the two evaluation tasks: sequential reaching (3D-star task) and activities of daily living (four ADL tasks). Our results find the manner of control space mapping (TS control versus JS control) to play a major role in both task performance and perceived workload.

A. Task Performance

More Intuitive vs. More Learnable. The performance results from the ADL tasks are shown in Figure 2. Over five days, we observe that both the TS group and JS group do improve in success rate. The initial performance of the JS group is superior to that of the TS group —specifically, on day 1, the JS group's median success rate is higher ($p < 0.05$, Wilcoxon signed-rank test) and median trial time is lower. However, only TS demonstrates statistically significant improvements, between days 1 and 5, in success rate ($p < 0.01$) and trial time ($p < 0.01$). Thus, TS control appears to have a *greater capacity for improvement*, as measured by task success and trial time, while JS control demonstrates *greater success with naïve use.*

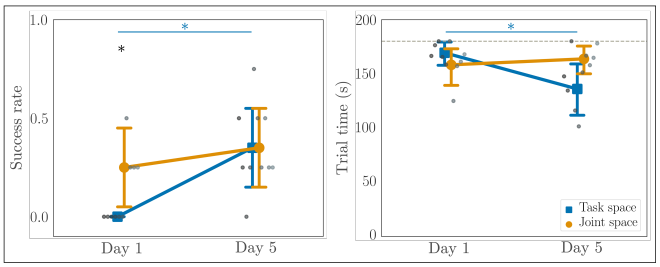

Fig. 2: Success rate (left) and trial time (right) for ADL tasks on first and last days. Grayscale dots represent the mean value for each participant (TS: dark; JS: light), and the dotted line (right) represents a timeout of 180 seconds. The standard interquartile ranges are shown. $^*p < 0.05$ (*within group).

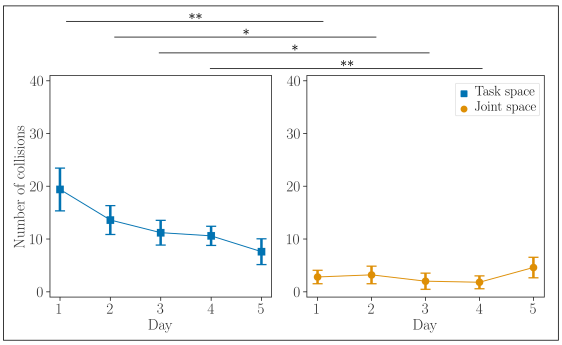

Fig. 3: Average number of collisions during the 3D-star task over five days. Standard deviation is shown. $^*p < 0.05$, $^{**}p < 0.01$ (*between groups).

Similarly, despite a noticeable early superiority in JS, on day 1, TS acheives a greater reduction in number of collisions in the 3D-star task compared to JS (days 1–4, $p < 0.05$; Kruskal-Wallis H-test), for which collision numbers remain largely static (Figure 3).

More (Room for) Improvement. Next, we evaluate success on the sequential reaching (3D-star) task. We examine how much time participants spend in workspace regions of interest: specifically, the proportion of time spent within 10% of the reach distance ($\tau_{dist\leq 10\%}$) and beyond 100% of the reach distance ($\tau_{dist\geq 100\%}$; farther from the target than is the starting position).[1] The results are shared in Figure 4. Note that while for an ideal reach, $\tau_{dist\geq 100\%}$ would be zero and $\tau_{dist\leq 10\%}$ minimized[c1]; *during learning*, an *increase* in $\tau_{dist\leq 10\%}$ is a marker of improvement when targets are not yet reachable. [c1]

We also observe that, on day one, both groups spend more

[1] A simple binary result of success is not informative, as no participants achieved the target location within our positional (1.00 cm) and rotational (0.02 rad or 1.14°) constraints on success. We also find the proportion of time metrics to be more informative than path length, for which no discernible trends emerge.

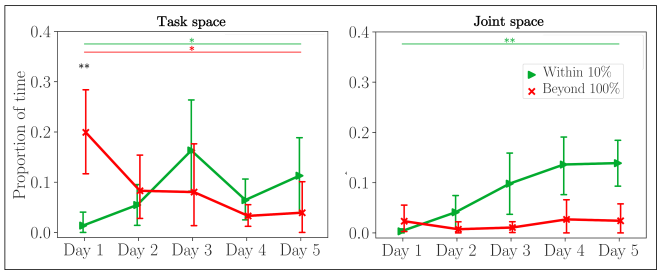

Fig. 4: Proportion of time the robot end-effector spends within 10% of reach distance (green) and outside of 100% of reach distance (red) in the 3D-star task. The standard interquartile ranges are shown. $^{*}p < 0.05$, $^{**}p < 0.01$ (*between categories, **within categories).

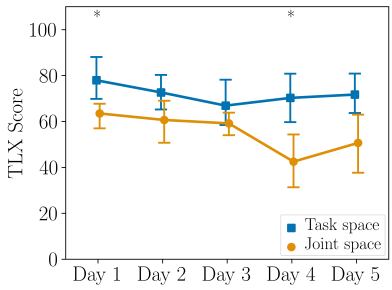

Fig. 5: Comparison of subjective workload, measured via NASA-TLX, between study groups. Evolution of NASA-TLX scores over study sessions. The standard interquartile ranges are shown. $^{*}p < 0.05$ (*between groups).

time beyond the starting distance (TS: 18 s; JS: 1.8 s) than near the targets (TS: 0.31 s; JS: 1.2 s). Both TS and JS groups significantly improve the amount of time spent near the targets ($\tau_{dist \leq 10\%}$) between days 1 and 5 ($p < 0.05$; Kruskal-Wallis H-test). TS also significantly reduces how much time is spent beyond the starting distance ($\tau_{dist \geq 100\%}$), between days 1 and 5 ($p < 0.05$), whereas this stays static in JS, largely due to having less room to improve.

B. Perceived Workload

A Different Sort of Learning. Figure 5 shows the NASA-TLX assessment and the evolution of scores for subjective workload across sessions. We observe a marked reduction over sessions in perceived workload (median NASA-TLX score) for the JS group. By contrast, we observe only a slight decrease in perceived workload for the TS group. Furthermore, the perceived workload of the JS group is consistently lower than that of the TS group across days, and even on day one, when the JS group's performance also was higher.

To evaluate statistical significance between the two groups, we initially use the Kruskal-Wallis H-test to find a main effect, and Conover's *post hoc* pairwise test, with Bonferroni adjustments, to make appropriate corrections. Only on days one and four do we find statistically significant differences between the two groups ($p < 0.05$).

We recall that the JS group did not improve much according to either of the ADL task performance metrics of success or trial time. While the JS group does not improve significantly in task performance, the group *does* improve in perceived workload—which perhaps is indicative of learning, albeit of a different sort than task performance learning (or at the very least familiarization).

Learning Takes Work. The TS group does not improve measurably with respect to perceived workload. This group, however, does improve according to both performance metrics, of success and trial time. Thus, a possible explanation is that the gains in performance are expensive to acquire—simply put, learning takes work.

V. Discussion

For individuals with paralysis, body-machine interfacing offers a promising path to increase functionality, by enabling them to directly teleoperate high-DoF assistive robots. To operate a BoMI requires learning a remapping of body movements to robot control signals. We have demonstrated this remapping within a 6D space to be learnable by an uninjured population, who were able to perform ADL tasks, in five days, under both control space mappings. Furthermore, this demonstration of 6D operation challenges the dimensionality mismatch problem that so often presents in the direct control of complex robotic arms, allowing for continuous and simultaneous operation of all robot control dimensions via the interface.

A focal question for our exploratory study was the feasibility of human learning to control high-DoF robots, continuously and simultaneously, using a BoMI. Although several prior studies [6] had demonstrated the ability of people with severe paralysis to use a BoMI to complete 2-DoF control tasks , other work had highlighted how challenging the control of additional DoFs can be, where 3-DoF control took 2–4 times longer to learn than 1-DoF or 2-DoF control, in a simple virtual reaching task [10]. Therefore, the overall learning burden was expected to be nontrivial, especially given the novelty of the interfacing and the non-anthropomorphic robotic arm.

We furthermore have found that a multi-session study was necessary to tease out our learning results. That is, a one-session study would have shown evidence that JS control was superior to TS control in operating high-DoF robots with a BoMI, and that TS control was unlearnable (Figures 2, 3, and 4). Instead, over five sessions, we have observed that TS control in fact was *more learnable* than JS control, which remained largely static over time. It moreover is likely that the TS group's task performance would have continued to improve in a longer study and that we have not yet shown the full capability of human learning on this system. We expect that further gains might be possible with a more regimented learning curriculum that further customizes the presentation of tasks and control access to each individual. Where the inflection point exactly lies on the human learning curve in TS control remains a topic for further investigation.

Our analysis of the role of control space mappings in learning high-dimensional BoMI and high-DoF robot control has provided evidence that *these mappings lead to different*

learning profiles (Figures 2, 3, and 4). A possible explanation for why participants in the JS group initially intuit robot control more is the comparative simplicity of single-joint movements. A similar phenomenon is observed in patients with cerebellar ataxia, where lesions in the cerebellum cause patients to think out individual joint movements rather than being able to coordinate multi-joint movements [22]. In addition, TS is forced to also learn the forward kinematics of the robotic arm (whereas JS did not).

Not only do the learning profiles differ with respect to task proficiency, they also differ in regards to *what was learned*. Learning is generally assessed with respect to task performance. Equally important within the field of assistive and rehabilitation robotics, however, is the burden on the human operator. Learning to interface with the robot with a lower workload also is learning, and it achieves one of the driving motivators for the development of assistive robots. Broadly, this is critical when such robots have had a history of acceptance issues by their users [23].

Lastly, a significant limitation to this work is that our investigation considers only uninjured populations. Recall that the key motivation for this work was to obtain a baseline understanding of the feasibility, scalability, and learnability of high-DoF robot teleoperation using a BoMI. While the BoMI previously had been shown to be effective at adjusting to the available residual movements in patients with cSCI (for 2D control) [6], questions related to the ability of human users to learn to teleoperate a robotic arm in high-DoFs using a BoMI, and whether control space mappings have any effect towards facilitating learning, were unanswered. Having now determined a baseline for human learning, our next steps will be to build on this work and apply the gained knowledge to a diverse population of patients with SCI.

VI. Conclusions

Individuals with paralysis can benefit from assistive robots and body-machine interfaces that help contribute to the return of their functionality and independence. In this paper, we share insights from a multi-session exploratory study that integrates body-machine interfacing with a high-DoF assistive robot and investigates human learning to control this system. Our most significant finding was the impact of the control space mapping from interface to robot control. While joint-space control was found to be *more intuitive* prior to training, task-space control was subject to greater improvement over time and thus presented as *more learnable* with respect to task proficiency. That said, workload reduction is another critical aspect to human learning to interface with robots, and, in this regard, joint-space control exhibited superior learning capacity. Therefore, there appears to be a trade-off between intuitiveness and learnability when comparing the two control space mappings. Both of these learning curves merit further investigations—with patients with motor impairments and with longer studies—that more deeply probe their potential points of inflections and plateaus.

Acknowledgment

Research reported in this publication was supported by the National Institute of Biomedical Imaging and Bioengineering (NIBIB), the NIH T32 Training Program and Eunice Kennedy Shriver National Institute Of Child Health & Human Development (NICHD), the National Science Foundation (NSF), National Institute on Disability, Independent Living and Rehabilitation Research (NIDILRR), and European Union's Horizon 2020 Research and Innovation Program under the Marie Sklodowska-Curie, Project REBoT. The content is solely the responsibility of the authors and does not necessarily represent the official views of the National Institutes of Health.

References

[1] K. Nas, L. Yazmalar, V. Şah, A. Aydın, and K. Öneş, "Rehabilitation of spinal cord injuries," *World J of Orthopedics*, vol. 6, no. 1, p. 8, 2015.
[2] J. L. Collinger, *et al.*, "High-performance neuroprosthetic control by an individual with tetraplegia," *The Lancet*, vol. 381, no. 9866, pp. 557–564, 2013.
[3] M. R. Tucker, *et al.*, "Control strategies for active lower extremity prosthetics and orthotics: a review," *J Neuroeng Rehabil*, vol. 12, no. 1, pp. 1–30, 2015.
[4] D. J. Rea and S. H. Seo, "Still not solved: A call for renewed focus on user-centered teleoperation interfaces," *Front Robot AI*, vol. 9, 2022.
[5] M. Casadio, R. Ranganathan, and F. A. Mussa-Ivaldi, "The body-machine interface: a new perspective on an old theme," *J Mot Behav*, vol. 44, no. 6, pp. 419–433, 2012.
[6] C. Pierella, *et al.*, "Learning new movements after paralysis: Results from a home-based study," *Sci Rep*, vol. 7, no. 1, pp. 1–11, 2017.
[7] F. Scholtes, G. Brook, and D. Martin, "Spinal cord injury and its treatment: current management and experimental perspectives," in *Adv Tech Stand Neurosurg*. Springer, 2012, pp. 29–56.
[8] M. Casadio, *et al.*, "Body machine interface: remapping motor skills after spinal cord injury," in *IEEE Int Conf Rehabil Robot (ICORR)*. IEEE, 2011, pp. 1–6.
[9] K. D. Anderson, "Targeting recovery: priorities of the spinal cord-injured population," *J Neurotrauma*, vol. 21, no. 10, pp. 1371–1383, 2004.
[10] R. Ranganathan, J. Wieser, K. M. Mosier, F. A. Mussa-Ivaldi, and R. A. Scheidt, "Learning redundant motor tasks with and without overlapping dimensions: facilitation and interference effects," *J Neurosci*, vol. 34, no. 24, pp. 8289–8299, 2014.
[11] L. V. Herlant, R. M. Holladay, and S. S. Srinivasa, "Assistive teleoperation of robot arms via automatic time-optimal mode switching," *ACM/IEEE Int Conf Hum-Robot Interact (HRI)*, pp. 35–42, 2016.
[12] A. Chari, S. Budhdeo, R. Sparks, D. G. Barone, H. J. Marcus, E. A. Pereira, and M. M. Tisdall, "Brain–machine interfaces: the role of the neurosurgeon," *World Neurosurg*, vol. 146, pp. 140–147, 2021.
[13] M. L. Martini, E. K. Oermann, N. L. Opie, F. Panov, T. Oxley, and K. Yaeger, "Sensor modalities for brain-computer interface technology: a comprehensive literature review," *Neurosurgery*, vol. 86, no. 2, pp. E108–E117, 2020.
[14] W. McKay, H. Lim, M. Priebe, D. Stokic, and A. Sherwood, "Clinical neurophysiological assessment of residual motor control in post-spinal cord injury paralysis," *Neurorehabil Neural Repair*, vol. 18, no. 3, pp. 144–153, 2004.
[15] D. De Santis, "A framework for optimizing co-adaptation in body-machine interfaces," *Front Neurorobot*, vol. 15, p. 662181, 2021.
[16] D. De Santis and F. A. Mussa-Ivaldi, "Guiding functional reorganization of motor redundancy using a body-machine interface," *J Neuroeng Rehabil*, vol. 17, no. 1, p. 61, 2020.
[17] F. Rizzoglio, M. Casadio, D. De Santis, and F. A. Mussa-Ivaldi, "Building an adaptive interface via unsupervised tracking of latent manifolds," *Neural Netw*, vol. 137, pp. 174–187, 2021.
[18] E. B. Thorp, *et al.*, "Upper body-based power wheelchair control interface for individuals with tetraplegia," *IEEE Trans Neural Syst Rehabil Eng*, vol. 24, no. 2, pp. 249–260, 2015.
[19] S. Chau, S. Aspelund, R. Mukherjee, M.-H. Lee, R. Ranganathan, and F. Kagerer, "A five degree-of-freedom body-machine interface for children with severe motor impairments," in *IEEE/RSJ International Conference on Intelligent Robots and Systems (IROS)*. IEEE, 2017, pp. 3877–3882.
[20] R. Shadmehr and F. A. Mussa-Ivaldi, "Adaptive representation of dynamics during learning of a motor task," *Journal of neuroscience*, vol. 14, no. 5, pp. 3208–3224, 1994.
[21] S. G. Hart, "Nasa-task load index (nasa-tlx); 20 years later," *Proc Hum Factors Ergon Soc*, vol. 50, no. 9, pp. 904–908, 2006.
[22] A. J. Bastian, T. Martin, J. Keating, and W. Thach, "Cerebellar ataxia: abnormal control of interaction torques across multiple joints," *J Neurophysiol*, vol. 76, no. 1, pp. 492–509, 1996.

[23] E. Biddiss and T. Chau, "The roles of predisposing characteristics, established need, and enabling resources on upper extremity prosthesis use and abandonment," *Disabil Rehabil Assist Technol*, vol. 2, no. 2, pp. 71–84, 2007.